Journal of Applied Polymer Science

# Crystallization behavior and morphology of polylactic acid (PLA) with aromatic sulfonate derivative

**Vidhya Nagarajan,[1,2] Amar K. Mohanty,[1,2] Manjusri Misra[1,2]**

[1]School of Engineering, Thornborough Building, University of Guelph, Guelph, ON N1G2W1, Canada

[2]Bioproducts Discovery and Development Centre, Department of Plant Agriculture, Crop Science Building, University of Guelph, Guelph, ON N1G2W1, Canada

Correspondence to: A. K. Mohanty (E-mail: mohanty@uoguelph.ca)

**ABSTRACT:** This article provides a detailed investigation of crystallization behavior and morphology of polylactic acid (PLA) in the presence of a nucleating agent: potassium salt of 5-dimethyl sulfoisothalate, an aromatic sulfonate derivative (Lak-301). Isothermal crystallization kinetics of PLA melt mixed with Lak at concentrations of 0.25–1 wt % was investigated at a range of crystallization temperature, 140–150 °C. To gain further insight on the effect of Lak, nonisothermal differential scanning calorimetry (DSC), wide angle X-ray diffraction (WAXD), polarized optical microscope (POM), heat deflection temperature (HDT), and rheology were also performed. At 0.25 wt % Lak, crystallinity of PLA increased from 10% to 45%, and in 1 wt % Lak, maximum crystallinity of 50% was achieved. With 1 wt % Lak, crystallization half time reduced to 1.8 min from 61 min for neat PLA at 140 °C. The isothermal crystallization kinetics was analyzed using Avrami model. Values of the Avrami exponent for PLA with Lak were mainly in the range of 3 indicating a three dimensional crystal growth is favored. Crystallization rate was found to increase with increase in Lak content. Observation from POM confirmed that the presence of Lak in the PLA matrix significantly increased the nucleation density. © 2016 Wiley Periodicals, Inc. J. Appl. Polym. Sci. **2016**, *133*, 43673.

**KEYWORDS:** biopolymers and renewable polymers; crystallization; kinetics; morphology; thermal properties

Received 29 November 2015; accepted 22 March 2016

**DOI: 10.1002/app.43673**

## INTRODUCTION

With global production of bioplastics forecast to quadruple by 2018,[1] there is a huge opportunity for major industries such as packaging, automotive, and construction, to meet their need for sustainable products using bioplastics. Polylactic acid (PLA) is a renewable resource-based compostable polymer having a favorable combination of material properties such as high strength and modulus, biocompatibility, and moderate barrier properties.[2] With comprehensive research and development efforts, PLA is increasingly becoming the sustainable material of choice for certain applications where conventional, nonbiodegradable polymers are used. Large scale availability at affordable cost due to advancements in manufacturing processes and increase in production capacity gives PLA an edge over other bioplastics. Much of the current research pertaining to PLA is directed toward overcoming its two major drawbacks: low impact strength and slow crystallization rate. Successful modification of these properties in cost efficient ways will greatly widen the use of PLA in packaging containers, agricultural, biomedical and engineering materials.

Depending on the D-lactide content, PLA can be either amorphous or crystalline. Melting temperature of semicrystalline PLA, with low content of D-lactide is in the range of 170–180 °C and glass transition temperature ($T_g$) is around 60 °C. Crystallization rate of semicrystalline PLA is very slow compared to other commercial polymers such as polypropylene and polyethylene.[3] Therefore, it is difficult to achieve high crystallinity without changes to formulation or processing conditions. PLA remains almost amorphous under practical processing and molding conditions adopted for injection molding processes with high rate of supercooling. Difficulty in demolding and ejection of parts made of PLA is also attributed to its slow crystallization. In the context of heat deflection temperature (HDT), increasing the crystallization rate of PLA is of great importance as higher amount of crystalline form contributes to high HDT at service temperatures above $T_g$.[4]

Major strategies that are known to increase the crystallinity of PLA are (1) formation of stereo-complex crystals, (2) use of nucleating agents, alone or in combination with plasticizers, (3) in some cases, epitaxy has also shown to be an effective way to speed crystallization of PLA.[5,6] Nucleation and crystallization

mechanisms are, however, different in each of these cases. Incorporation of a nucleating agent is the most economical and widely used method for accelerating the crystallization process and increasing the crystallinity content. Presence of a nucleating agent in a virgin polymer can influence the kinetics and crystalline morphology by offering nucleation sites for initializing the crystallization process.[7] Lowering the crystallization half time with the addition of a nucleating agent can help shorten the molding cycle times. Numerous investigations have been conducted on improving the crystallization of PLA.[8–26] Anderson *et al.*[8] investigated the nucleating efficiency of stereo complex in comparison with talc, a common nucleating agent. In their study, crystallization half time of PLA was reduced to less than 1 min with addition of 6% of talc, however, the stereocomplex showed a superior effect compared to talc.[8] Liao *et al.*[9] investigated the effect of three different nucleating agents, $CaCO_3$, $TiO_2$, and $BaSO_4$ (0.5–2.0 wt %) and studied their isothermal crystallization kinetics. $BaSO_4$ at 0.5 wt % was concluded to have maximum effect on crystallization of PLA. Tsuji *et al.*[10] ordered the acceleration effects of various nucleating agents on the crystallization of poly(L-lactic acid) PLLA in decreasing order as: poly(D-lactic acid)- > talc > fullerence C60 > montmorillonite > polysaccharides. Nofar *et al.*[11] investigated the crystallization behavior of linear and long chain branched PLA and their crystallization kinetics. Blending PLA with polymers having higher crystallization rate can result in blends with improved crystallinity. Blends of PLA with polyglycolide, polyoxymethylene (POM), polyhydroxy butyrate (PHB), poly ε-caprolactone (PCL) have been proved to possess improved crystallization rate compared to neat PLA.[12–14] Numerous other nucleating agents like talc,[15] N,N′-ethylene bis-stearamide (EBS),[16] carbon nanotubes,[17] zinc phenyl phosphate,[18] multiamide and hydrazide compounds,[10,19–24] nano-calcium carbonate (CaCO3),[25] and orotic acid[26] have also been examined in PLA.

In this article, we have investigated the effectiveness of an aromatic sulphonate derivative (potassium salt of 5-dimethyl sulfoisothalate), commercially available as Lak-301 in increasing the crystallization rate of PLA. In our previous publication,[27] we showed that use of Lak in combination with high molding temperature had helped in improving the crystallinity and hence the HDT of PLA biocomposites. We also concluded Lak offered best results in comparison to other nucleating agents such as precipitated calcium carbonate and magnesium oxysulfate. Recently, Shi *et al.*[28] investigated the synergistic effect of polyethylene glycol (PEG) plasticizer in combination with Lak, talc, $CaCO_3$, and halloysite nanotubes. They concluded Lak and talc provided better enhancement of PLA crystallization in comparison to other nucleating agents. To the best of our knowledge, isothermal crystallization kinetics and nucleation behavior of Lak at different concentration in PLA have not been investigated in detail. Intent of this article is, therefore, to investigate the effect of Lak concentration, crystallization temperature on the overall crystallization rate, and crystallizability of PLA with Lak.

## EXPERIMENTAL

### Materials and Sample Preparation

PLA, Ingeo 3001D with 1.5% D-lactide content was purchased from NatureWorks LLC, USA. Potassium salt of 5-dimethyl sulfoisothalate commercially available as Lak-301 was purchased from Takemoto Oil & Fat Co, Japan. Nucleating agent will be referred as Lak in the article. Neat PLA was oven-dried at 80 °C for at least 12 hrs. Samples of neat PLA and PLA with different concentrations of Lak (0.25, 0.5, 0.75, and 1 wt %) were fabricated through melt extrusion and injection molding. 15 cc, co-rotating twin screw micro extruder and 12 cc micro injection molding machine (DSM Research, Netherlands) were used. Processing temperature of 180 °C, screw RPM of 100, and residence time of 2 min was adopted for all the samples. Melt from the extruder was collected and transferred to the injection molder through a preheated collecting device. Holding pressure and time was set to 9 bar and 18s, respectively. Samples were molded to disc shape for rheology testing at a molding temperature of 30 °C. Neat PLA was also processed under identical conditions to possess similar thermal history.

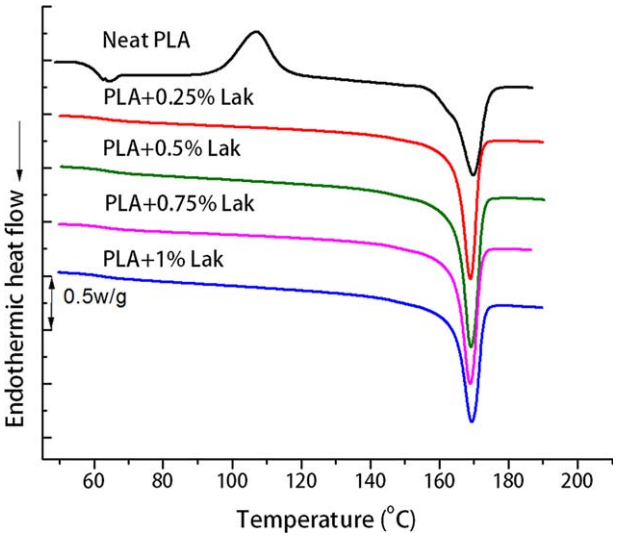


**Figure 1.** DSC melting traces of PLA and PLA with Lak from second heating cycle. [Color figure can be viewed in the online issue, which is available at wileyonlinelibrary.com.]

### Testing and Characterization

**Differential Scanning Calorimetry (DSC).** Nonisothermal DSC was performed under heat-cool-heat cycle. Heating profile of 0-190 °C with heating rate of 10 °C/min was adopted for first and second heat cycle. Isothermal hold of 3 min was included between cycles to erase the thermal history. Cooling cycle was run at 5 °C/min. Isothermal DSC was performed by heating the samples to 190 °C with heating rate of 10 °C/min followed by isothermal step at desired crystallization temperature for 30 mins. Samples of 3–5 mg for both isothermal and nonisothermal DSC were prepared from specimens molded at 30 °C. TA Instruments (New Castle, DE) DSC Q200 was used for the analysis.

**Wide Angle X-ray Diffraction (WAXD).** WAXD profiles of the samples were collected at room temperature from SuperNova Agilent single-crystal diffractometer equipped with a microfocus CuKα ($\lambda = 1.54184$ Å) radiation source and Atlas CCD detector. X-Ray diffraction images were collected from four different angular positions of the goniometer using $\varphi$-scans to generate a 1D powder pattern within $2\theta$ range of 5° and 100°. Images were

**Table I.** Thermal Characteristics of PLA and PLA with Different Concentration of Lak

| Sample | $T_m$ (°C) | $\Delta H_m$ (J/g) | $T_{cc}$ (°C) | $T_c$ (°C) | $T_g$ (°C) | $\chi_c$ (%) |
|---|---|---|---|---|---|---|
| Neat PLA | 169.5 ± 0.1 | 41.1 ± 0.1 | 117.8 ± 0.2 | 105.3 ± 0.3 | 63.0 ± 0.3 | 10.6 ± 0.3 |
| PLA + 0.25% Lak | 168.9 ± 0.3 | 40.9 ± 0.1 | - | 132.3 ± 0.2 | 62.9 ± 0.1 | 44.8 ± 0.2 |
| PLA + 0.5% Lak | 168.9 ± 0.1 | 40.1 ± 0.2 | - | 133.6 ± 0.4 | 62.9 ± 0.1 | 45.1 ± 0.4 |
| PLA + 0.75% Lak | 169.1 ± 0.2 | 41.8 ± 0.1 | - | 134.2 ± 0.2 | 62.7 ± 0.2 | 48.3 ± 0.1 |
| PLA + 1% Lak | 169.7 ± 0.3 | 42.8 ± 0.2 | - | 134.6 ± 0.2 | 62.6 ± 0.1 | 50.8 ± 0.2 |

processed using CrysAlisPro software. Plots of the powder pattern were generated from the original images with a step of 0.02° in $2\theta$.

**Heat Deflection Temperature (HDT).** Dynamic Mechanical Analyzer (DMA) Q800 from TA Instruments was used for measuring the HDT by heating the samples at 2 °C/min under a pre-load force calculated to match 0.455 MPa as per ASTM D648. HDT reported is the temperature corresponding to 0.1889% strain; results are an average of two samples.

**Scanning Electron Microscope (SEM).** Phenon ProX (Phenon World BV, Netherlands) SEM equipped with a back scattering electron (BSE) detector was used to study the morphology of PLA samples with nucleating agent. Processed, nonisothermal samples were used for the analysis.

**Polarized Optical Microscope (POM).** POM from Nikon Instruments Inc., Canada equipped with a hot stage from Linkam Scientific Instruments Ltd., UK was used to perform a qualitative analysis of the crystallization process. Samples were melted at 180 °C, and a maximum cooling rate of 50 °C/min was used to bring the samples to desired isothermal temperature.

**Rheological Characterization.** Anton Paar MCR302 rheometer (Anton Paar GmbH, Graz, Austria) with a parallel plate configuration (22 mm plate and 1 mm measurement gap) under nitrogen atmosphere was used for rheological characterization. Frequency sweep analysis was done between 0.1–600 rad/s, at 190 °C and 1% strain rate.

## RESULTS AND DISCUSSION

### Nonisothermal Crystallization Behavior

Effect of Lak on crystallization of PLA under nonisothermal conditions were studied and the DSC thermograms of melting from second heating cycle for neat PLA and PLA with increasing concentration of Lak are presented in Figure 1.

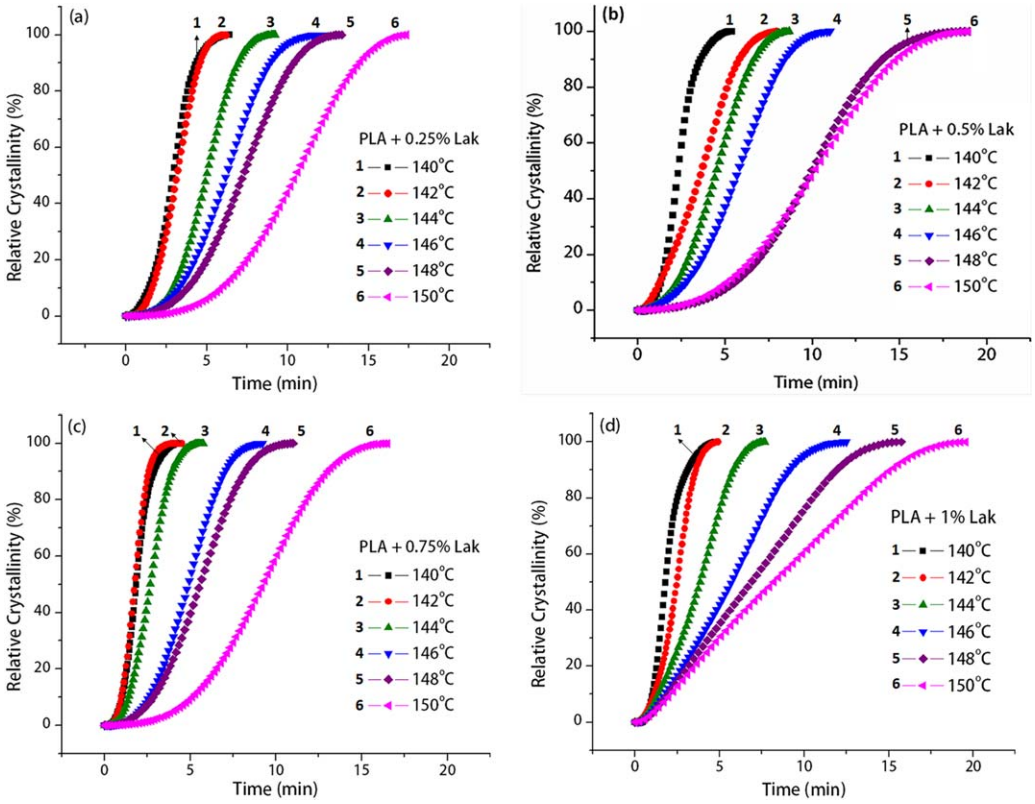


**Figure 2(a–d).** Relative crystallinity plots for PLA with different wt % of Lak. [Color figure can be viewed in the online issue, which is available at wileyonlinelibrary.com.]

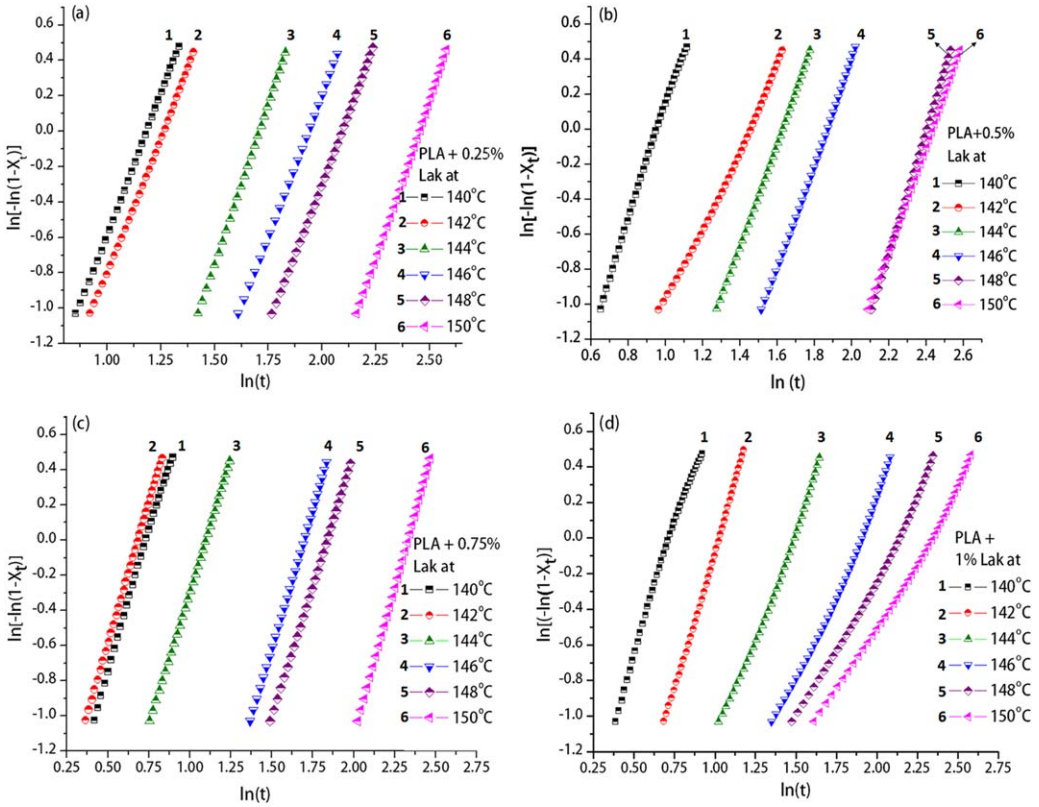


**Figure 3(a–d).** Avrami Plots for PLA with different wt % of Lak. [Color figure can be viewed in the online issue, which is available at wileyonlinelibrary.com.]

Melting ($T_m$), cold crystallization ($T_{cc}$), and crystallization ($T_c$) peak temperatures, melting enthalpy ($\Delta H_m$), glass transition temperature ($T_g$), and percentage crystallinity ($\chi_c$) calculated from second heating cycle are provided in Table I. PLA exhibited its characteristic cold crystallization, melting peaks, and glass transition temperature ($T_g$). First obvious observation from Figure 1 is the cold crystallization peak which reflects the materials ability to crystallize below the melting temperature. The presence of cold crystallization peak in the second heating cycle of neat PLA indicates some of the semicrystalline chains were still capable of rearranging or recrystallizing before melting. The absence of cold crystallization peak in PLA/Lak is a good indication Lak acts as an effective nucleating agent in promoting the crystallization process.

In previously published literature on crystallization of PLA with other nucleating agents, reduction in cold crystallization peak and in some cases disappearance has been reported and this behavior has been concluded to signify the efficiency of nucleating agent in enhancing the crystallization process.[20,24] The crystallization peak temperature, $T_c$ of PLA showed drastic improvement from 105 °C to 134 °C with the addition of Lak. Also, $T_c$ showed an increasing trend with increasing concentration of Lak again suggesting Lak is an efficient nucleating agent, supported by literature.[20,24,26] Presence of nucleating agent favors heterogeneous nucleation which would decrease the free enthalpy and increase the nucleation rate in the high temperature region and shift the $T_c$ value to higher temperature.[29] Percentage crystallinity ($\chi_c$) of PLA and PLA/Lak formulations were calculated using the equation,

$$\chi_c = \frac{\Delta H_m - \Delta H_{cc}}{f.\Delta H_m^0} * 100\% \quad (1)$$

$\Delta H_m$ is the melting enthalpy and $\Delta H_{cc}$ is cold crystallization enthalpy, both taken from second heating cycle. $\Delta H_m^0$ is 100% crystalline PLA's melting enthalpy, 93.7 J/g,[30] and $f$ corresponds to the weight fraction of PLA. With the disappearance of cold crystallization peak in the presence of Lak, crystallinity as high as 50% was achieved. Like $T_c$, percentage crystallinity also showed an increasing trend with increase in Lak concentration.

### Isothermal Crystallization Kinetics

Isothermal crystallization behavior of PLA with different levels of Lak was examined at a range of temperatures between 140 °C and 150 °C. Literature suggests the crystallization temperature of PLA to be in the range of 105 °C–120 °C.[3,8,9] In this study, we have selected 120 °C and 140 °C as isothermal crystallization temperature ($T_{c\text{-iso}}$) for pure PLA. In the case of PLA containing Lak, it was difficult to conduct the isothermal study at temperatures less than 140 °C as some of the crystals were already formed at temperatures below 140 °C while cooling from melt condition, even when a maximum cooling rate of 50 °C was used. When the polymer melt is rapidly cooled from melt to predetermined $T_{c\text{-iso}}$, there is a time interval before the start of crystallization. This time is termed induction time, during which nucleation and growth process has been suggested to take place. Efficient nucleating agent shortens the induction time and enhances the overall rate of transformation from the molten state to the crystalline solid state. For instance, in the case of PLA with 1% Lak, induction time was noticed to be 2s at 140 °C, whereas for neat PLA,

**Table II.** Isothermal Crystallization Kinetics Parameter Obtained from Avrami Plots

| Sample | ln(k)-intercept | *k* | Standard error | *n* (slope) | Standard error | Half Time ($t_{1/2}$) |
|---|---|---|---|---|---|---|
| **Neat PLA** | | | | | | |
| 120°C | −4.8 | 0.007 | 0.004 | 2.1 | 0.002 | 8.3 |
| 140°C | −10.1 | 0.000 | 0.000 | 2.4 | 0.002 | 60.8 |
| **PLA + 0.25% Lak** | | | | | | |
| 140°C | −3.7 | 0.023 | 0.003 | 3.1 | 0.002 | 2.9 |
| 142°C | −3.8 | 0.020 | 0.004 | 3.0 | 0.004 | 3.1 |
| 144°C | −6.1 | 0.002 | 0.001 | 3.6 | 0.001 | 4.9 |
| 146°C | −6.1 | 0.002 | 0.003 | 3.1 | 0.002 | 6.2 |
| 148°C | −6.7 | 0.001 | 0.003 | 3.2 | 0.001 | 7.2 |
| 150°C | −8.7 | 0.000 | 0.004 | 3.5 | 0.002 | 10.5 |
| **PLA + 0.5% Lak** | | | | | | |
| 140°C | −3.1 | 0.044 | 0.006 | 3.2 | 0.007 | 2.3 |
| 142°C | −3.2 | 0.038 | 0.007 | 2.2 | 0.005 | 3.6 |
| 144°C | −3.3 | 0.035 | 0.007 | 1.8 | 0.004 | 5.1 |
| 146°C | −5.5 | 0.004 | 0.004 | 2.9 | 0.002 | 7.6 |
| 148°C | −8.4 | 0.000 | 0.002 | 3.5 | 0.001 | 9.9 |
| 150°C | −7.3 | 0.001 | 0.003 | 3.0 | 0.001 | 10.1 |
| **PLA + 0.75% Lak** | | | | | | |
| 140°C | −2.3 | 0.098 | 0.004 | 3.1 | 0.006 | 1.8 |
| 142°C | −2.2 | 0.110 | 0.002 | 3.2 | 0.002 | 1.9 |
| 144°C | −3.3 | 0.036 | 0.002 | 3.0 | 0.002 | 2.6 |
| 146°C | −5.3 | 0.005 | 0.003 | 3.1 | 0.002 | 4.8 |
| 148°C | −5.5 | 0.004 | 0.002 | 3.0 | 0.001 | 5.5 |
| 150°C | −7.8 | 0.000 | 0.003 | 3.3 | 0.001 | 9.2 |
| **PLA + 1% Lak** | | | | | | |
| 140°C | −2.0 | 0.127 | 0.009 | 2.8 | 0.013 | 1.8 |
| 142°C | −3.1 | 0.041 | 0.005 | 3.1 | 0.005 | 2.4 |
| 144°C | −3.5 | 0.028 | 0.010 | 2.3 | 0.007 | 3.8 |
| 146°C | −3.8 | 0.021 | 0.010 | 2.0 | 0.005 | 5.7 |
| 148°C | −3.5 | 0.028 | 0.007 | 1.6 | 0.004 | 6.8 |
| 150°C | −3.5 | 0.030 | 0.005 | 1.5 | 0.002 | 8.2 |

induction time was 6 min at 120 °C. Such shortening of induction times in the presence of Lak is understandable, as PLA does not have to undergo self-nucleation.

Isothermal crystallization can be better understood by evaluating the relative degree of crystalline conversion or relative crystallinity ($X_t$) as a function of time at different crystallization temperatures selected. Relative crystallinity is expressed as the ratio of the area of the crystallization time, *t*, to the total area of the exotherm peak,

$$X_t = \frac{\int_0^t (dH/dt)dt}{\int_0^\infty (dH/dt)dt} \quad (2)$$

Where, $dH/dt$ is the rate of heat flow during the crystallization process at time *t*.

F2 Figure 2(a–d) shows the evolution of relative crystallinity with time for PLA with different levels of Lak at a range of isothermal crystallization temperatures. Sigmoid nature of the relative crystallinity curves, with time dependence is obvious. These figures clearly depict the increase in crystallization time as the crystallization temperature increases from 140 °C to 150 °C. There is a critical $T_{c\text{-iso}}$ where the crystallization rate is the fastest. Below this critical temperature, the crystallization rate is dominated by crystal nucleation and above this critical temperature crystal growth rate is the dominant mechanism due to the increase in molecular mobility.[31]

Avrami theory is the most common and widely used method to analyze and describe the isothermal crystallization kinetics. Avrami method relates relative crystallinity, $X_t$, to crystallization time, *t*, by the equation,

$$1 - X_t = \exp\ (-kt^n) \quad (3)$$

$$\text{or } \ln[-\ln(1-X_t)] = n\ \ln(t) + \ln(k) \quad (4)$$

Where *k* is the crystallization rate constant involving both nucleation and growth rate parameters. *n* is the Avrami exponent,

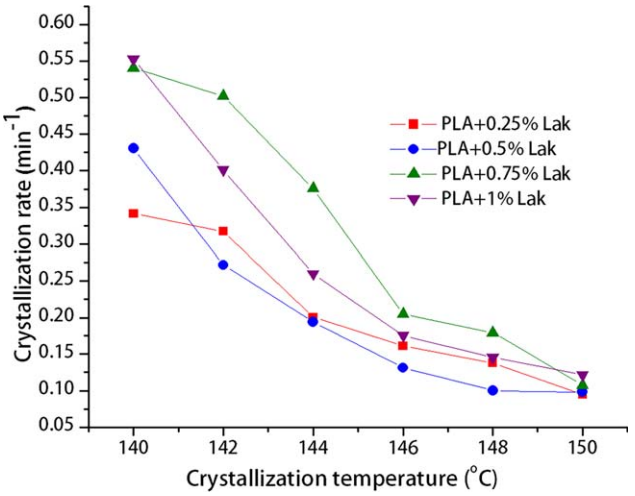


**Figure 4.** Crystallization rate vs crystallization temperature for PLA with Lak. [Color figure can be viewed in the online issue, which is available at wileyonlinelibrary.com.]

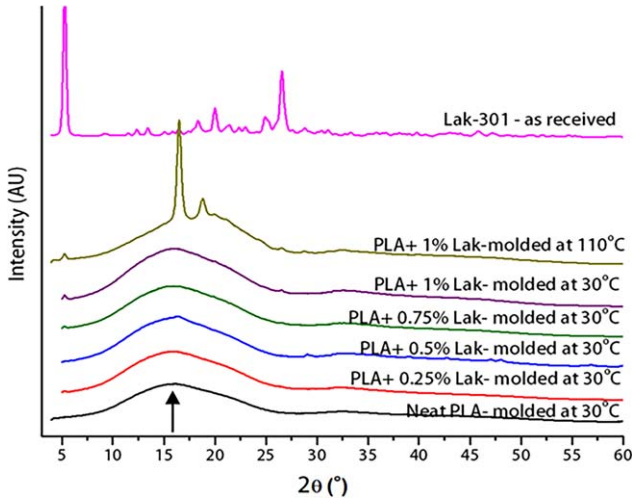


**Figure 5.** WAXD pattern for meat PLA and PLA with different concentration of Lak. [Color figure can be viewed in the online issue, which is available at wileyonlinelibrary.com.]

dependent on the nature of nucleation and crystal growth dynamics.[26] By plotting ln {ln[1 $X(t)$]} versus ln(t), the Avrami exponent $n$, and the logarithm of the kinetic constant ln $k$, can be determined from the slope and intercept, respectively. In general, these double log plots show deviations from linearity toward the beginning and end of crystallization due to initial and secondary crystallization.[20] Secondary crystallization is considered to occur due to crystal perfection and/or impingement of spherulites.[29] Therefore, only 20%–80% of relative crystallinity linear portion data was used to fit the equation to obtain $n$ and $k$ values.

F3 Avrami plots ln {ln[1 $X(t)$]} versus ln(t) for PLA with different concentrations of Lak at a range of crystallization temperatures is shown in Figure 3(a–d). Almost parallel nature of the lines for a given sample in these plots indicates a good fit. Results evaluated from the plots are summarized in Table II. For neat PLA, the values of $n$ range from 2.1 to 2.4 which are similar to literature values of 2.1–2.4 at $T_{c\text{-}iso}$ = 120 °C–140 °C by Xu *et al.*[24]; 2.0–2.3 at $T_{c\text{-}iso}$ = 114 °C–126 °C by Zhang *et al.*[32]; 2.5–2.9 at $T_{c\text{-}iso}$ = 90 °C–140 °C by Tsuji *et al.*[33]; 2.4–2.8 at $T_{c\text{-}iso}$ = 120 °C–140 °C by Weng *et al.*[34] In case of PLA with Lak, the $n$ values have shifted from the range of 2 for pure PLA to range of 3 with 0.25, 0.5, and 0.75% Lak and back to the range of 1.5–3 for PLA with 1% Lak. This strongly indicates conditions such as, presence of the nucleating agent Lak, its concentration, and the crystallization temperature, have strong influence on the crystallization mechanism of PLA. Avrami exponent, $n$ usually range from 1–4, the lower values (1–2) are associated with two dimensional growth with instantaneous and sporadic nucleation while the higher $n$ values (3–4) denotes three dimensional growth of spherulites with just sporadic or combination of simultaneous and sporadic nucleation.[35] $n$ values in the range of 2 obtained for pure PLA indicates mainly homogeneous nucleation with two dimensional crystal growth was favored in the absence of nucleating agents. $n$ values in the range of 3 obtained for PLA with 0.25%, 0.5%, and 0.75% Lak indicates that at particular concentration of Lak, three dimensional crystal growth is favored.

The drop in $n$ value with increase in Lak concentration (1%) can be attributed to increased nucleation density which could result in a large number of partially developed spherulites impinging with each other at very early stage of crystallization thus resulting in sheaf like structures or truncated spherulites. Presence of such intermediate sheaf like crystal geometry has been reported to decrease the Avrami exponent from 3.[36,37] k values with unit $min^{-n}$ are dependent on $n$, and $n$ varies with $T_{c\text{-}iso}$, therefore, $k$ values are not directly compared. Hence, crystallization kinetics is discussed based on crystallization half time ($t_{1/2}$), crystallization rate ($\tau_{1/2}$), and activation energy. Crystallization half time, $t_{1/2}$ is defined as the time required to achieve

**Table III.** HDT for PLA/Lak formulations Molded at Different Temperatures

| PLA/Lak formulations at different mold temperatures | HDT (°C) |
|---|---|
| PLA + 0.25% Lak at 30°C | 56.1 ± 0.2 |
| PLA + 0.5% Lak | |
| 30°C | 56.1 ± 0.3 |
| 60°C | 56.8 ± 0.1 |
| 90°C | 58.0 ± 0.2 |
| 110°C | 88.3 ± 0.3 |
| PLA + 0.75% Lak | |
| 30°C | 56.1 ± 0.1 |
| 60°C | 56.2 ± 0.1 |
| 90°C | 58.7 ± 0.2 |
| 110°C | 116.0 ± 0.2 |
| PLA + 1% Lak | |
| 30°C | 56.2 ± 0.1 |
| 60°C | 56.4 ± 0.2 |
| 90°C | 58.7 ± 0.1 |
| 110°C | 140.8 ± 1.2 |

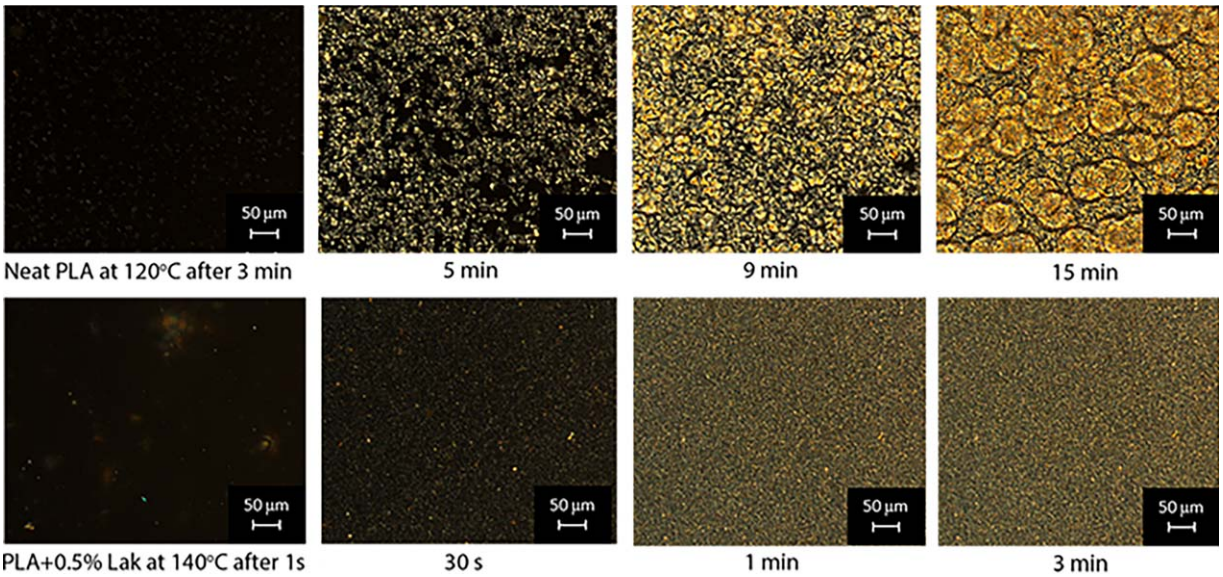


**Figure 6.** Polarized optical microscopy images of PLA (top row) and PLA with 0.5% Lak (bottom row) at 20× magnifications. [Color figure can be viewed in the online issue, which is available at wileyonlinelibrary.com.]

50% of the final crystallinity of the sample at a given $T_{c\text{-iso}}$, expressed by the equation

$$T_{1/2}=(\ln 2/k)^{1/n} \quad (5)$$

The reciprocal of $t_{1/2}$ is denoted as the crystallization rate, $\tau_{1/2}$. Parameter $k$ is a temperature-dependent factor; it is denoted in the Arrhenius form for isothermal transformation as

$$\ln(k)=\ln(k_0)-\frac{E}{RT} \quad (6)$$

The activation energy for overall crystallization can be determined by plotting $\ln(k)$ vs $1/T$ and $\ln(k)$ is directly related to the activation energy. For neat PLA, the $\ln(k)$ value is $-10.7$ at 140 °C, comparing this to PLA with Lak, the $\ln(k)$ values and thus the activation energy is reduced in the presence of Lak. Another notable point is the increase in $\ln(k)$ value (activation energy) of PLA/Lak with increase in crystallization temperature. Calculated values of $t_{1/2}$ are listed in Table II.

With the addition of Lak the crystallization half time reduced significantly and showed an increasing trend with increase in crystallization temperature. Lowest crystallization half time was achieved for PLA with 1% Lak at 140 °C. These observations suggest Lak is effective in enhancing the isothermal crystallization behavior of PLA and the level of improvement is dependent on the crystallization temperature. Based on the explanations of Gao *et al.*[38] and Kang *et al.*[39] the change in $t_{1/2}$ with the addition of nucleating agent is based on the nucleation rate which is controlled by free enthalpy of formation of nuclei of critical size, and free energy of the activation governs the diffusion of polymer segments across the phase boundary. In the high temperature region, free enthalpy is the dominant factor controlling nucleation rate; whereas in the low temperature region, free energy of activation has a greater influence on the nucleation rate. They have attributed higher $t_{1/2}$ of neat PLA to high free enthalpy and hence slow crystallization. With the addition of nucleating agent, free enthalpy reduces which in turn enhances primary nucleation. For more clarity, dependence of crystallization rate ($\tau_{1/2}$) on isothermal crystallization temperature is explained by plotting $1/t_{1/2}$ as a function of $T_{c\text{-iso}}$ in Figure 4.

It is clear from this graph that the crystallization rate is gradually decreasing with increase in $T_{c\text{-iso}}$ and a progressive increase is observed with increase in the concentration of Lak. At temperatures between 142 °C and 148 °C, 0.75% Lak shows higher crystallization rate compared to PLA with 1% Lak. These observations suggest Lak is effective in accelerating the overall isothermal crystallization process.

### Wide Angle X-ray Diffraction (WAXD)

In order to study the effect of addition of Lak on the crystal forms of PLA, WAXD patterns were recorded for neat PLA and PLA with different Lak content, and they are shown in Figure 5. Depending on different crystallization conditions, PLA is known to crystallize in three different crystal modifications: α, β, and γ forms.[40,41] Among the three crystal forms, α form is the most commonly observed crystal structure for crystals developed from melt crystallization at $T_c$ higher than 120 °C, and α' form for $T_c$ less than 100 °C.[40–42] In our study, samples were not crystallized and the WAXD pattern obtained reflect the crystallization structure developed during processing of samples at the specified molding conditions (30 °C and 110 °C). From Figure 5, it is evident that neat PLA exhibited a broad hollow ascribed to the amorphous nature and a weak reflection peak at $2\theta = 16.84°$, revealing the semicrystalline nature. Addition of Lak at different levels did not change this behavior, however a slight increase in the intensity of the peak was observed with increase in the concentration of Lak from 0.25% to 1%. With increase in mold temperature to 110 °C, Lak enhanced the crystallization of PLA and hence two strong peaks appeared at $2\theta = 16.84°$ and $2\theta = 19.1°$. These two peaks indexed as (200/

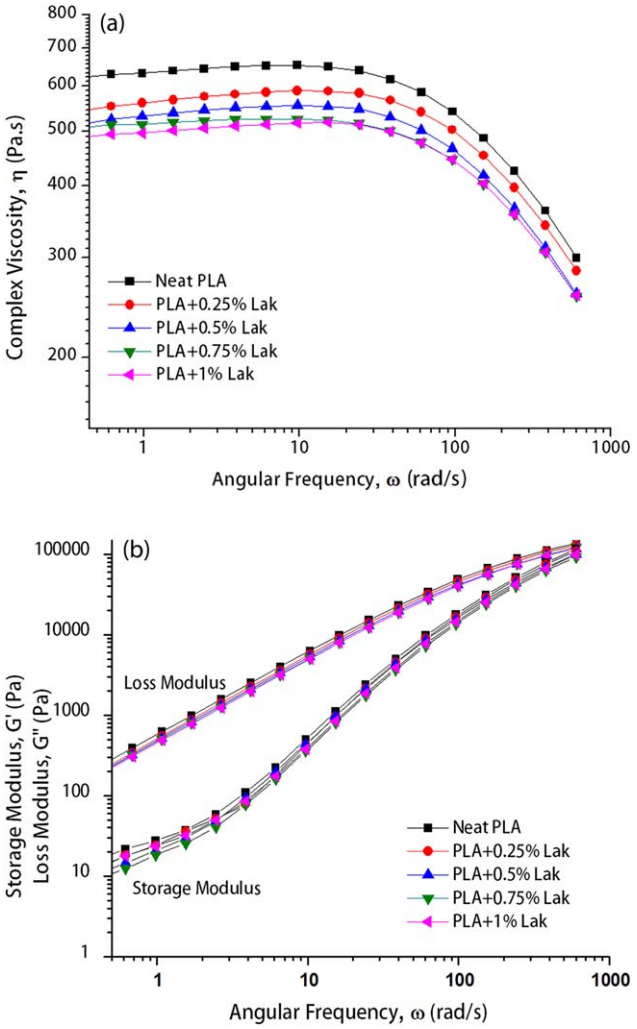


**Figure 7(a–b).** Variation in complex viscosity, storage modulus, and loss modulus of PLA/Lak with increasing Lak content as a function of frequency. [Color figure can be viewed in the online issue, which is available at wileyonlinelibrary.com.]

110) and (203) are characteristic peaks for a typical α and α' crystal forms of PLA.[24]

### Heat Deflection Temperature (HDT)

As discussed in the Introduction section, adding nucleating agents to improve the crystallization of PLA is one of the efficient ways to improve the short term heat resistance property of PLA indicated by HDT. Current study along with other published literature has established the effectiveness of Lak-301 in improving the crystallinity of PLA; hence it is natural to expect that it would also significantly improve the HDT. However, in spite of successful enhancement in crystallization rate of PLA through addition of nucleating agents, obtaining injection molded articles of PLA with high crystallinity remains difficult due to very high mold cooling rate. HDT results obtained in this study, presented in Table III, also support this practical limitation of using Lak for samples molded at low mold temperature. Main reason for this observation is the insufficient level of crystallinity developed in nucleated PLA molded at room temperature with fast cooling rates typically higher than 100 °C/min. As mold temperature is increased, tremendous improvements are observed and an increasing trend in HDT was observed in samples containing higher amounts of Lak molded at 110 °C. Based on the targeted applications, suitable molding conditions have to be adopted for desired HDT in final formulations. These results further corroborate with crystallinity profiles obtained from WAXD.

### Spherulite Morphology from Optical Microscopy

In the case of neat PLA, nucleation and subsequent crystal growth was difficult to observe at temperatures higher than 130 °C, where as in the case of PLA containing nucleating agent Lak, the crystals were already partially formed at this temperature while cooling from melt state. Therefore, the optical microscope images shown in Figure 6 were captured at 120 °C for neat PLA and 140 °C for PLA with Lak. Images for only PLA with 0.5% Lak are shown as similar crystallization behavior was noted invariable of the content of Lak. At melt state, optical microscopy image for PLA was completely dark but in other formulations with Lak, the Lak particles were actually visible as bright spots as shown in Figure 6(b). Nucleation and spherulites growth occurred rather slowly in neat PLA compared to PLA containing nucleating agents. The spherulites sizes were large and were impinging on each other. An efficient nucleating agent is expected to provide a surface conducive to nucleation and increase the nucleation density by reducing the surface free energy barrier for primary nucleation.[29] Based on the above explanation, Lak can be an effective nucleating agent as the nucleation density increased with much smaller spherulites size but with larger number of spherulites. The crystallization appears to be complete by 3–4 min in the presence of Lak at 140 °C. These observations further confirm that incorporation of Lak is a promising means to improve the crystallization of PLA at appropriate molding conditions.

### Rheology

Rheology is of fundamental and practical interest as it can reveal changes in macromolecular chain structure with the addition of nucleating agents based on the variation in melt viscosity. Figure 7(a–b) presents the storage modulus (G') and complex viscosity ($\eta$) of neat PLA and PLA/Lak formulations at 190 °C as a function of angular frequency. Complex viscosity of PLA and PLA with Lak exhibited Newtonian behavior at lower frequencies and shear thinning behavior at higher frequencies. It can be seen, at lower frequencies, complex viscosity of PLA containing Lak was less than neat PLA and this behavior was pronounced at concentrations of 0.75% and 1% Lak. Such reduction in complex viscosity could be attributed to reduction in free volume as the nucleating agent increases the crystallinity of PLA, or just the presence of Lak particles which could interfere with physical process of chain entanglements in PLA melt. Similar behavior has been reported previously by other researchers in nucleated systems with PLA as matrix.[43,44] The storage modulus, G' and loss modulus G" of PLA with Lak was almost the same as neat PLA and at certain concentrations slightly lower than PLA. A characteristic terminal flow behavior of $G'(\omega) \propto \omega^2$ and $G''(\omega) \propto \omega$ was expected for PLA and it was observed to follow this behavior fairly well. The slopes of

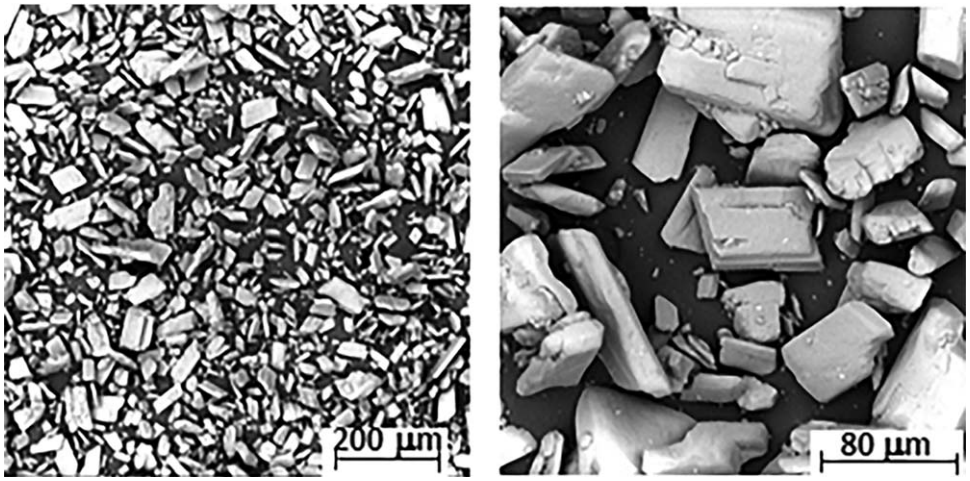


**Figure 8.** SEM Images of Lak-301 at 200× and 1000× magnification.

$G'(\omega)$ and $G''(\omega)$ calculated from angular frequencies lower than 10 rad/s for neat PLA was 1.93 and 0.96, respectively. These values are consistent with values reported by other researchers for PLA.[43–45] Addition of Lak did not seem to affect the shape and slope of storage modulus and loss modulus curves indicating chain dynamics were not drastically affected by the presence of Lak.

### Scanning Electron Microscopy (SEM)

SEM of Lak-301 is shown in Figure 8 at low and high magnifications. Irregular trapezoidal crystal structures with particle size ranging from approximately 5–200 $\mu$m were observed. Some of the large size particles were noticed to be agglomerated. Fractured surface morphology of PLA with Lak is shown in Figure 9. The fractured surface was obtained by breaking the extruded strands of PLA containing different concentrations of Lak. SEM micrographs on the top row show the distribution of Lak particles in PLA matrix. As the concentration of Lak is increased, more particles were seen on the surface, and hence a propensity for higher nucleation density. At 0.25% Lak concentration, the fracture surface of PLA is smooth, characteristic of PLA brittle fracture. As the concentration increased to 1%, a rough fracture surface with some fibrils was observed. SEM micrographs in the bottom row show the development of spherulites structures in PLA/Lak formulations. The sizes of the spherulites were in the order of 100 $\mu$m. The spherulites observed here seems to have formed from an aggregate of lamellae radiating from the center outward. They appear to have a Lak particle as a central nucleating entity which has initiated the crystal growth in all directions. Thus, the different crystals are nucleated separately and grow uncorrelated. Also, the spherulites developed have distinct boundaries, and are noticed to impinge on each other. The size of the spherulite is reduced and is smaller in the case of PLA with 1% Lak. Another notable observation is spherulitic structures which have formed only around certain Lak particles. This could be due to the wide range of variation in the Lak particle size or simply not enough time to undergo complete crystallization process under the adopted processing conditions. This SEM morphology shown here gives an idea of

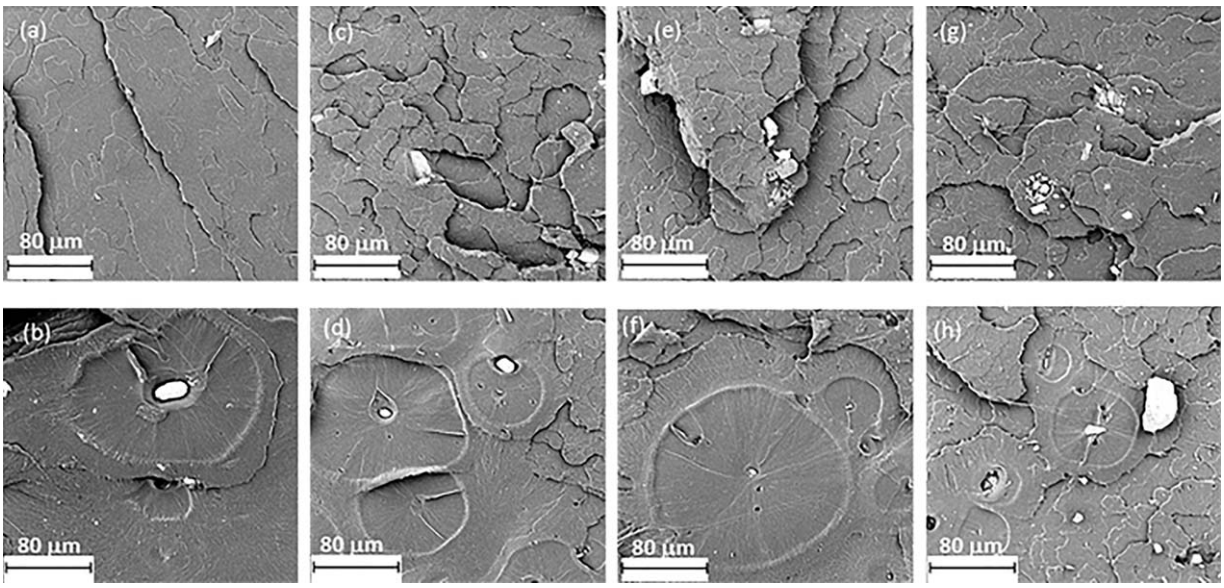


**Figure 9.** SEM Images of (a,b) PLA + 0.25% Lak; (c,d) PLA + 0.5% Lak; (e,f) PLA + 0.75% Lak; (g,h) PLA + 1%Lak at 1000× magnification.

the morphology that is likely to develop in PLA formulations under nonisothermal conditions with fairly high cooling rates from melt temperature.

## CONCLUSIONS

PLA with different concentration of Lak was prepared through melt extrusion and injection molding. The isothermal and nonisothermal crystallization behavior, isothermal crystallization kinetics, spherulitic morphology, and crystalline structure of PLA and PLA with Lak were investigated in detail. The addition of even small amounts of Lak significantly enhanced the nonisothermal crystallization peak temperature of PLA from 105 °C to 134 °C. The isothermal crystallization kinetics study revealed the overall crystallization rate to be much faster in PLA nucleated with Lak and the rate was found to be highest at 0.75 wt % Lak. Crystallization rate, however, decreased with increasing crystallization temperature indicating the presence of critical isothermal crystallization temperature. Crystallization half time as low as 1.8 min was obtained while adding 0.75%–1% Lak at isothermal crystallization temperature of 140 °C. The values of the Avrami exponent of the neat PLA indicated two dimensional crystal growths. In the case of PLA/Lak formulations, at Lak concentration of up to 0.75% the *n* values were around 3 indicating a three dimensional crystal growth. With further increase in Lak concentration to 1 wt % Avrami exponent value reduced, this is believed to be due to increased nucleation density which could result in a large number of partially developed spherulites impinging on each other. Therefore, at early stage of crystallization sheaf like structures or truncated spherulites are expected to be developed. The observations from POM showed greater nucleation density in PLA/Lak blends with numerous small size spherulites compared to larger and sparse spherulite structures developed in PLA. WAXD profiles showed both neat PLA, and PLA with Lak was having mainly α and α' form of crystal structure and hence we can conclude Lak did not modify the crystal structure but enhanced the process of crystallization. In summary, Lak can be effective in providing the required crystallizability for PLA, which could help in extending the practical range of PLA applications, when the products are molded at higher molding temperature.

## ACKNOWLEDGMENTS

The authors gratefully acknowledge the financial support from (1) the Ontario Ministry of Agriculture, Food, and Rural Affairs (OMAFRA)- University of Guelph Bioeconomy Industrial Uses Theme (Project # 200425); (2) the Ontario Ministry of Economic Development and Innovation (MEDI), Ontario Research Fund, Research Excellence Round 4 program (ORF-RE04) (Project # 050231 and 050289); and (3) the Natural Sciences and Engineering Research Council (NSERC) Canada Discovery Grants (Project # 400322) and Networks of Centres of Excellence of Canada (NCE) AUTO21 program (Project # 460372).

## REFERENCES

1. European Bioplastics, Institute for Bioplastics and Biocomposites, nova-Institute, 2014. Available at: http://en.european-bioplastics.org/market/, Accessed on 4 November, **2015**.
2. Auras, R. A.; Lim, L.; Selke, S. E.; Tsuji, H. Poly (Lactic Acid): Synthesis, Structures, Properties, Processing, and Applications; Wiley: New York, **2011**.
3. Schmidt, S. C.; Hillmyer, M. A. *J. Polym. Sci., Part B: Polym. Phys.* **2001**, *39*, 300.
4. Li, M.; Hu, D.; Wang, Y.; Shen, C. *Polym. Eng. Sci.* **2010**, *50*, 2298.
5. An, Y.; Jiang, S.; Sun, J.; Chen, X. *Chin. J. Polym. Sci.* **2011**, *29*, 513.
6. Tu, C.; Jiang, S.; Li, H.; Yan, S. *Macromolecules* **2013**, *46*, 5215.
7. Saeidlou, S.; Huneault, M. A.; Li, H.; Park, C. B. *Prog. Polym. Sci.* **2012**, *37*, 1657.
8. Anderson, K. S.; Hillmyer, M. A. *Polymer* **2006**, *47*, 2030.
9. Liao, R.; Yang, B.; Yu, W.; Zhou, C. *J. Appl. Polym. Sci.* **2007**, *104*, 310.
10. Tsuji, H.; Takai, H.; Fukuda, N.; Takikawa, H. *Macromol. Mater. Eng.* **2006**, *291*, 325.
11. Nofar, M.; Zhu, W.; Park, C. B.; Randall, J. *Ind. Eng. Chem. Res.* **2011**, *50*, 13789.
12. Guo, X.; Liu, H.; Zhang, J.; Huang, J. *Ind. Eng. Chem. Res.* **2014**, *53*, 16754.
13. Tsuji, H.; Sawada, M.; Bouapao, L. *ACS Appl. Mater Interfaces* **2009**, *1*, 1719.
14. Tri, P. N.; Domenek, S.; Guinault, A.; Sollogoub, C. *J. Appl. Polym. Sci.* **2013**, *129*, 3355.
15. Yu, F.; Liu, T.; Zhao, X.; Yu, X.; Lu, A.; Wang, J. *J. Appl. Polym. Sci.* **2012**, *125*, E99.
16. Tang, Z.; Zhang, C.; Liu, X.; Zhu, J. *J. Appl. Polym. Sci.* **2012**, *125*, 1108.
17. Barrau, S.; Vanmansart, C.; Moreau, M.; Addad, A.; Stoclet, G.; Lefebvre, J.; Seguela, R. *Macromolecules* **2011**, *44*, 6496.
18. Han, Q.; Wang, Y.; Shao, C.; Zheng, G.; Li, Q.; Shen, C. *J. Compos. Mater.* **2014**, *48*, 2737.
19. Bai, H.; Zhang, W.; Deng, H.; Zhang, Q.; Fu, Q. *Macromolecules* **2011**, *44*, 1233.
20. Song, P.; Wei, Z.; Liang, J.; Chen, G.; Zhang, W. *Polym. Eng. Sci.* **2012**, *52*, 1058.
21. Gui, Z.; Lu, C.; Cheng, S. *Polym. Test* **2013**, *32*, 15.
22. Xu, T.; Wang, Y.; Han, Q.; He, D.; Li, Q.; Shen, C. *J. Macromol. Sci., Part B: Phys.* **2014**, *53*, 1680.
23. Kawamoto, N.; Sakai, A.; Horikoshi, T.; Urushihara, T.; Tobita, E. *J. Appl. Polym. Sci.* **2007**, *103*, 244.
24. Xu, T.; Zhang, A.; Zhao, Y.; Han, Z.; Xue, L. *Polym. Test* **2015**,
25. Liang, J.; Zhou, L.; Tang, C.; Tsui, C. *Composites, Part B* **2013**, *45*, 1646.
26. Qiu, Z.; Li, Z. *Ind. Eng. Chem. Res.* **2011**, *50*, 12299.
27. Nagarajan, V.; Zhang, K.; Misra, M.; Mohanty, A. K. *ACS Appl. Mater. Interfaces* **2015**, *7*, 11203.
28. Shi, X.; Zhang, G.; Phuong, T. V.; Lazzeri, A. *Molecules* **2015**, *20*, 1579.
29. Kai, W.; He, Y.; Inoue, Y. *Polym. Int.* **2005**, *54*, 780.

30. Yasuniwa, M.; Sakamo, K.; Ono, Y.; Kawahara, W. *Polymer* **2008**, *49*, 1943.

31. Hu, W. In Polymer Physics: A Molecular Approach; Hu, W., Ed.; Polymer Crystallization. Springer: Vienna, **2013**, pp 187–221.

32. Zhang, R.; Wang, Y.; Wang, K.; Zheng, G.; Li, Q.; Shen, C. *Polym. Bull.* **2013**, *70*, 195.

33. Tsuji, H.; Takai, H.; Saha, S. K. *Polymer* **2006**, *47*, 3826.

34. Weng, M.; Qiu, Z. *Thermochim. Acta* **2014**, *577*, 41.

35. Battegazzore, D.; Bocchini, S.; Frache, A. *eXPRESS Polym. Lett.* **2011**, *5*, 8.

36. Muellerleile, J. T.; Risch, B. G.; Rodrigues, D. E.; Wilkes, G. L.; Jones, D. M. *Polymer* **1993**, *34*, 789.

37. Lee, Y.; Porter, R. S. *Macromolecules* **1988**, *21*, 2770.

38. Gao, X.; Liu, R.; Jin, M.; Bu, H. *J. Polym. Sci., Part B: Polym. Phys.* **2002**, *40*, 2387.

39. Kang, K. S.; Lee, S. I.; Lee, T. J.; Narayan, R.; Shin, B. Y. *Korean J. Chem. Eng.* **2008**, *25*, 599.

40. Zhang, J.; Duan, Y.; Sato, H.; Tsuji, H.; Noda, I.; Yan, S.; Ozaki, Y. *Macromolecules* **2005**, *38*, 8012.

41. Pan, P.; Inoue, Y. *Prog. Polym. Sci.* **2009**, *34*, 605.

42. Zhang, J.; Tashiro, K.; Tsuji, H.; Domb, A. *J. Macromolecules* **2008**, *41*, 1352.

43. Gu, S.; Zou, C.; Zhou, K.; Ren, J. *J. Appl. Polym. Sci.* **2009**, *114*, 1648.

44. Luo, Y.; Li, W.; Wang, X.; Xu, D.; Wang, Y. *Acta Mater.* **2009**, *57*, 3182.

45. Ray, S. S.; Yamada, K.; Okamoto, M.; Ueda, K. *Polymer* **2003**, *44*, 857.